Impact of body part thickness on AP pelvis radiographic image quality and effective dose

K. Alzyoud [a, b, *], P. Hogg [a], B. Snaith [c, d], K. Flintham [c], A. England [a]

[a] School of Health Sciences, University of Salford, Salford M6 6PU, United Kingdom
[b] Faculty of Allied Health Sciences, Hashemite University, Zarqa, Jordan
[c] The Mid Yorkshire Hospitals NHS Trust, Wakefield WF1 4DG, United Kingdom
[d] University of Bradford, Bradford BD7 1DP, United Kingdom

ARTICLE INFO

ABSTRACT

Introduction: Within medical imaging variations in patient size can generate challenges, especially when selecting appropriate acquisition parameters. This experiment sought to evaluate the impact of increasing body part thickness on image quality (IQ) and effective dose (E) and identify optimum exposure parameters.

Methods: An anthropomorphic pelvis phantom was imaged with additional layers (1–15 cm) of animal fat as a proxy for increasing body thickness. Acquisitions used the automatic exposure control (AEC), 100 cm source to image distance (SID) and a range of tube potentials (70–110 kVp). IQ was evaluated physically and perceptually. E was estimated using PCXMC software.

Results: For all tube potentials, signal to noise ratio (SNR) and contrast to noise ratio (CNR) deceased as body part thickness increased. 70 kVp produced the highest SNR (46.6–22.6); CNR (42.8–17.6). Visual grading showed that the highest IQ scores were achieved using 70 and 75 kVp. As thickness increases, E increased exponentially ($r = 0.96$; $p < 0.001$). Correlations were found between visual and physical IQ (SNR $r = 0.97$, $p < 0.001$; CNR $r = 0.98$, $p < 0.001$).

Conclusion: To achieve an optimal IQ across the range of thicknesses, lower kVp settings were most effective. This is at variance with professional practice as there is a tendency for radiographers to increase kVp as thickness increases. Dose reductions were experienced at higher kVp settings and are a valid method for optimisation when imaging larger patients.

Introduction

A number of challenges exist when imaging obese patients, not only in the challenges around table weight limits.[1–8] Moreover, radiographers may experience difficulties in transporting and positioning patients together with identifying anatomical landmarks necessary for accurate radiographic centring. In relation to IQ, beam attenuation, low levels of image contrast, lengthy exposure times and motion artefacts are further issues.[4]

Image quality (IQ) is likely to be compromised when imaging obese people. As the thickness of the body part under investigation increases the quantity of scattered radiation increases.[6] A number of techniques exist which can sustain IQ, either by increasing the tube current–time product (mAs), inclusion of a grid or automatic exposure control (AEC).[6] However, increasing the mAs and including a grid results in an increase radiation dose.[5] An alternative approach is to use high tube potentials, but this decreases the image contrast and could adversely affect diagnosis.[6] Understanding the optimum combination of mAs and kVp, when imaging large patients is poorly understood. The aim of this study was to assess the impact of increasing body part thickness on IQ and effective dose (E), and to identify optimum exposure parameters when imaging patients of different sizes during pelvis radiography.

Methods

This phantom based study was conducted at the University of Salford (Ethical approval – HSR1617-142).

* Corresponding author. University of Salford, School of Health Sciences, Salford M6 6PU, United Kingdom.
E-mail addresses: k.alzyoud@edu.salford.ac.uk (K. Alzyoud), p.hogg@salford.ac.uk (P. Hogg), bev.snaith@midyorks.nhs.uk (B. Snaith), kevin.flintham@midyorks.nhs.uk (K. Flintham), a.england@salford.ac.uk (A. England).

Imaging equipment and technique

Before starting the study, quality assurance testing was conducted in accordance with IPEM Report 91[9]; results fell within expected tolerances. A Wolverson Arcoma Arco Ceil general radiography system (Arcoma, Annavägen, Sweden) together with a Caesium Iodide (CsI) AeroDR image detector (Konica Minolta Medical Imaging USA INC, Wayne, NJ, USA) was used. This image capture system had an image area of 35 × 43 cm with a 1994 × 2430-pixel matrix, pixel size was 175 μm. Within the table Bucky there was an anti-scatter radiation grid (grid ratio 10:1, 40 lines/cm).

An adult lower sectional torso RS-113T anthropomorphic pelvis phantom (Radiology Support Devices, Long Beach, CA) was positioned supine. A fixed collimation field was used with beam centring in the midline, halfway along an imaginary line connecting the anterior superior iliac spines and the symphysis pubis.[10]

Obesity was simulated by adding fat equivalent material. Our method was a simplification of the "apples" and "pears" distributions more typically observed in adult body types.[5,11,12] This would be where the additional body fat would predominantly accumulate in the anterior structures. Many studies have simulated additional soft tissue material either above or below the phantom.[13,14] Commercially available animal fat (lard) was placed inside a rectangular plastic box placed on the anterior surface of the phantom (Fig. 1). The rationale for using a plastic box was that this was the simplest, and most consistent way to position the fat over the phantom and was also a practical way to add fat in 1 cm increments. Commercially available catering lard was used as the fat equivalent material.[15–18] Validity was established by analysing the computed tomography (CT) density of the fat using a similar method described by Yoshizumi et al.,[19] and comparing it against human tissue. The CT density ranged from −78 to −80 Hounsfield unit (HU). Data from the literature reported that the mean ± standard deviation (SD) CT density for abdominal fat, across a range of ages and body compositions, was −93 ± 25 HU.[19]

Study acquisition parameters were based on local clinical protocols and the literature.[20–22] A control image (no additional fat, both outer AEC chambers, table Bucky, 100 cm SID, no additional filtration and 80 kVp) were used. The resultant image was considered as the reference image for IQ evaluation. Following this, 144 experimental images were acquired, with 1–15 cm of additional fat (1 cm increments), a range of tube potentials (70–110; 5 kVp intervals). All other exposure conditions, including the AEC configuration, remained constant and images were processed using an anteroposterior (AP) pelvis algorithm which would be used during clinical imaging.

Dosimetry

Three exposures were performed for each experimental setup. To minimise random error, three Dose Area Product (DAP) readings were recorded. E was calculated using the Monte Carlo software PCXMC 2.0 (STUK, Radiation and Nuclear Safety Authority, Helsinki, Finland). In order to accurately simulate the differences in body part thicknesses the source to skin distance (SSD) was measured for each fat thickness. With the simulations the weight of the phantom was modified for each one cm increase in fat thickness (one kg increase per 0.96 cm increase in AP diameter). This formula was based on the study conducted by Miyatake[23] assuming a linear relationship between increasing waist circumferences and weight.[24,25] Moreover, increasing phantom size was not shown to affect the position of internal organs and that they would only be covered by layers of adipose tissue.[26]

Image quality assessment

Visual image quality

A relative visual grade assessment (VGA) method was first selected since it provides the ability to measure subtle changes in IQ. Relative VGA, using bespoke software,[27–32] allowed the comparison of two images simultaneously. This image comparison method has been previously described.[32] Two images were displayed side-by-side, one being the reference image and the other the experimental image under evaluation. Observers were invited to evaluate images using a validated visual scale consisting of 15 criteria (Table 1).[33] For each image, observers independently graded the different criteria using a 5-point Likert scale (much better, better, the same, worst or much worse than the reference image). Images were presented to participants on two five-megapixel DOME E5 (NDSsi, Santa Rosa, CA) monitors (2048 by 2560 pixels). Monitors were calibrated to the grey scale digital imaging and communications in medicine (DICOM) standard.[34] Observers consisted of six qualified radiographers with clinical experience ranging from 5 to 10 years. Basic vision acuity checks were undertaken on each participant[35] and all observers were blinded to the acquisition parameters. Room lighting was dimmed and maintained at a constant luminance of >170 cd/m^2.[36]
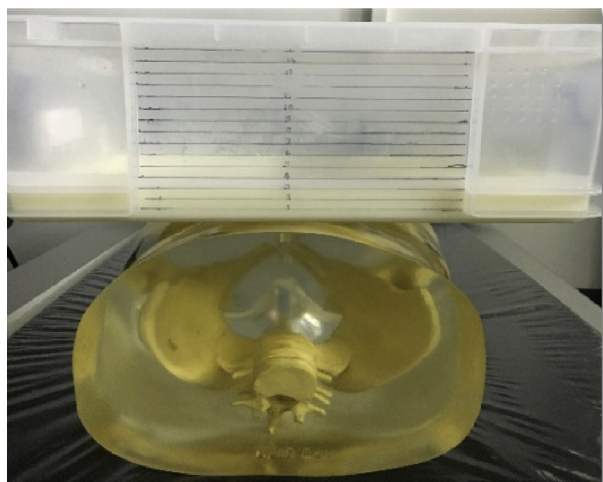

Figure 1. Experimental setup of the pelvis phantom and additional fat container (scaled 1 cm increments in a plastic box).

Table 1
Criteria used for the visual grading.[33]

Item	Criteria
Anatomical region	The left hip joint is adequately visualised.
	The right hip joint is adequately visualised.
	The left lesser trochanter is visualised adequately.
	The right lesser trochanter is visualised adequately
	The left greater trochanter is visualised adequately
	The right greater trochanter is visualised adequately
	The right sacro-iliac joint is adequately visualised.
	The left iliac crest is visualised adequately.
	The right iliac crest is visualised adequately
	Left acetabulum is visualised clearly
	Right acetabulum is visualised clearly.
	The pubic and ischial rami are not adequately visualised.
	The both femoral necks are visualised adequately
	The medulla and cortex of the pelvis are adequately demonstrated.
	There is a significant amount of noise in this image.

Absolute grading was also chosen to provide a definitive opinion on whether images were acceptable for diagnostic purposes, thus reflecting clinical practice. Two radiographers, each with more than ten years of reporting experience made a binary decision as to whether images were suitable for diagnosis (yes or no). Within this process, using their professional experience, they considered five anatomical areas which has previously been used for evaluating pelvis X-ray images, these include:

- Sacro iliac joints (assessing integrity/ankylosis)
- Iliacs (bilaterally) (bony lesions)
- Pubic rami (insufficiency fractures/lesions)
- Hip joints bilaterally (OA)
- Proximal femora – suggest intertrochanteric line (bony lesions)

Physical image quality

Signal to noise ratio (SNR) and contrast to noise ratio (CNR) have been used successfully in similar IQ studies.[37–40] Four region of interest (ROIs) were drawn in homogeneous structures on the resultant images, ROIs were positioned in the locations as described by Bloomfield et al.[41] (Fig. 2). Two ROIs were drawn in the iliac region and a further two in the femoral region. Both the iliac and femoral regions were evaluated separately. ROI1 would be the mean signal from either both iliac crest regions or from both femoral head regions. We opted to present data from only one region (femora) since both areas generated very similar trends and this simplified the data for analysis. Two further ROIs were selected to represent the background (noise). In order to sample the mean and standard deviation of the pixel values on the images, the computer software ImageJ (National Institutes of Health, Bethesda, MD) was used. ImageJ has previously been used for IQ assessments,[42,43] SNR and CNR were calculated using the following equations[40,44,45]:

$$CNR = \frac{ROI_1 - ROI_2}{\sigma_2}$$

$$SNR = \frac{mean\ signal}{\sigma_{noise}}$$

where ROI_1 is the mean signal from the area of interest (anatomy) and ROI_2 is the mean signal from the noise.
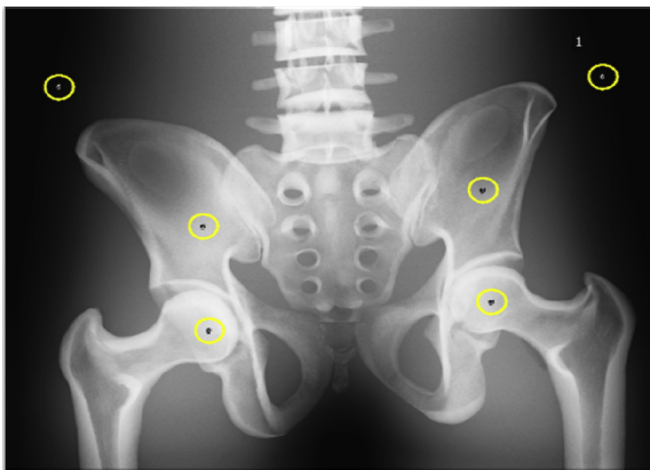

Figure 2. Illustrates the four different ROIs (circles) used for the SNR and CNR calculations together with the two background ROIs used to indicate image noise.

σ_2 was calculated as $\sqrt{(SD1)^2 + (SD2)^2/2}$[44] where SD1 and SD2 are the standard deviation for region 1 and 2 of noise.

Statistical analysis

All data were inputted into SPSS Version 22.0 (IBM Inc, Armonk, NY) for analysis. Study results showed a normal distribution using the Shapiro–Wilk test,[46,47] this was with the exception of optimisation score. Pearson's r and scattered plots were generated to investigate correlations between the relative VGA and physical IQ. All data were expressed as percentage change values relative to the reference image. Inferential analyses, between different tube potentials were undertaken using analysis of variance (ANOVA). P values <0.05 were considered to be statistically significant. Interobserver variability was assessed using an inter-class correlation coefficient (ICC).

Results

The ICC for all six observers was 0.91 (95%CI 0.88–0.93) indicating a high level of agreement.[48,49]

Radiation dose

E for the reference image (80 kVp) was 0.012 mSv. However, for the same kVp, with an additional 15 cm fat, this increased by 856% to 1.13 mSv. At 110 kVp, E was the lowest for all fat thicknesses (0.0 cm fat, 0.06 mSv vs 15 cm fat, 0.43 mSv [646% increase]). E was highest using 70 kVp; with 0 cm fat where it was 0.17 mSv, this increased by 1371% when compared to the reference image (1.73 mSv for 15 cm of additional fat).

Among all fat thicknesses there were significant differences in E across all tube potentials, from 70 kVp to 110 kVp (p < 0.05). As fat thickness increases, E increased exponentially (r = 0.96, p < 0.001; Fig. 3).

IQ assessment

Physical image quality

For all kVp values, SNR and CNR decreased as fat thickness increased (r = −0.6 to −0.8; p ≤ 0.01) (Figs. 4 and 5). 70 kVp had the highest SNR (46.6 at 0 cm and 22.6 at 15 cm) and CNR (42.9 at 0 cm and 17.6 at 15 cm). The lowest SNR was at 110 kVp, 30.2 at 0 cm and 19.6 at 15 cm. The smallest decrease in SNR was at 70 kVp (−106%) across all thicknesses. A similar trend was noted for the CNR but the decrease was greater than that of SNR. When adding 15 cm of additional fat and when using 110 kVp CNR decreased by 64% compared to 50% for SNR.

Visual image quality

Relative VGA showed the highest IQ scores for acquisitions at 70 kVp and 75 kVp. The highest score was at 70 kVp (57.5) and the lowest at 110 kVp (15.0) for all thicknesses (Fig. 6). There was a strong positive correlation between SNR/CNR and E (0.99 & 0.99, respectively; p < 0.001). The correlation between E and visual IQ score was r = 0.98 (p < 0.001). Results indicate that there was a strong correlation between physical and visual IQ scores (SNR *vs* visual IQ score r = 0.97, p < 0.001; CNR *vs* visual IQ score r = 0.98, p < 0.001). For the binary image decision task (diagnostically acceptable – Yes/No), all images were deemed adequate for diagnosis by both reporting radiographers.

Effective dose

E increased as body part thicknesses increased (r = 0.96; p < 0.001), with highest values at 70 and 75 kVp (0.17 and 0.13 mSv,
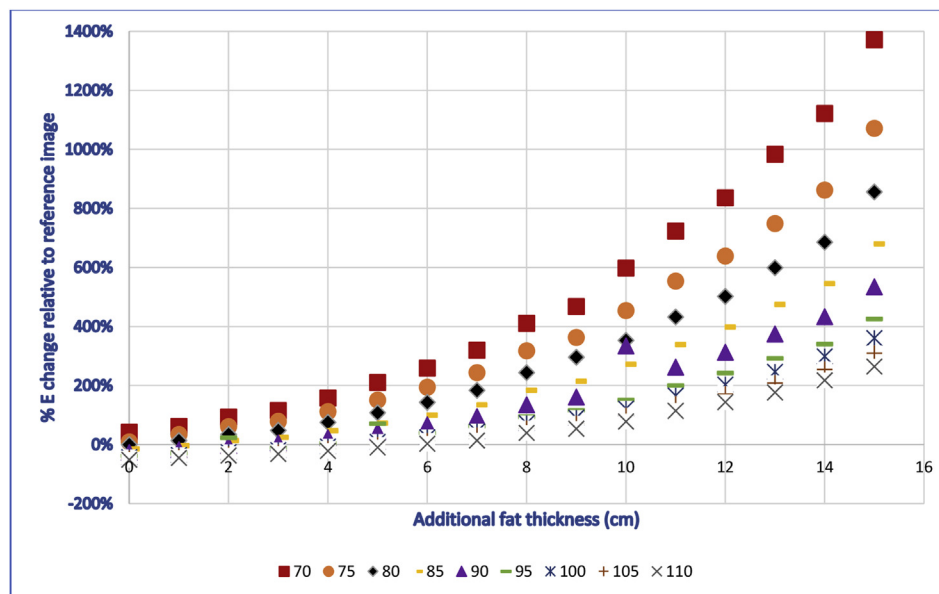
Figure 3. Percentage change of E relative to the reference image (80 kVp) for all body part thicknesses. Values in the figure legend correspond to the respective tube potentials.
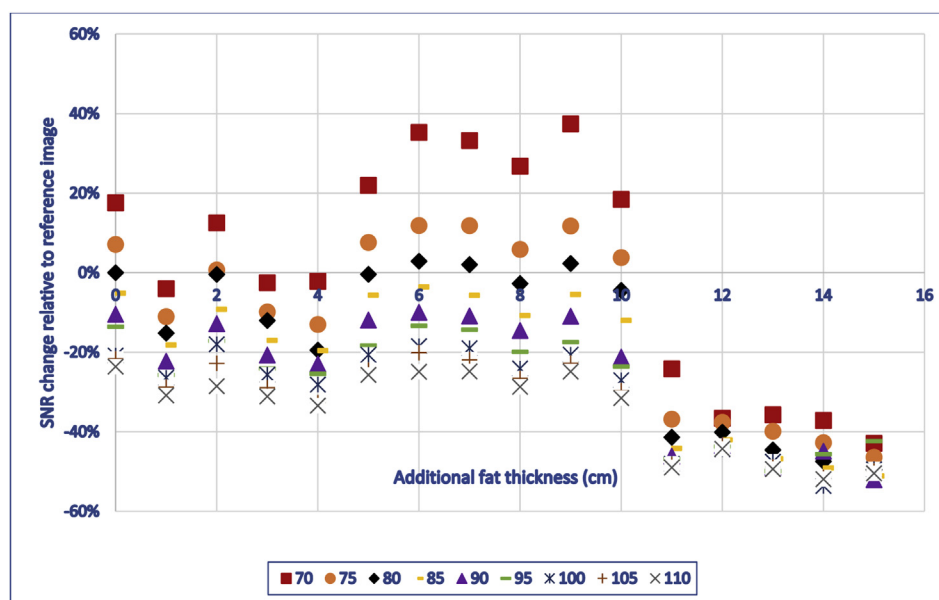

Figure 4. Percentage change of SNR relative to the reference image (80 kVp) for all body part thicknesses. Values in the figure legend correspond to the respective tube potentials.

respectively), whereas high tube potentials generated the lowest E (Fig. 3).

Discussion

Results from our study indicate that when imaging larger people there needs to be additional modification to radiographic technique. Visual IQ was highest at 70 kVp (57.5), for all body part thicknesses, this does not reflect typical clinical practice where practitioners commonly increase the tube potential as thickness increases. At high kVps (105 & 110) there was approximately a 68% reduction in IQ relative to the reference image. Reductions in IQ at higher kVps could be expected due to the anticipated reductions in contrast and increases in scattered radiation. Importantly, the

results from our study raise questions regarding the justification for increasing the tube potential as body part thickness increases.

Similar findings were encountered when reviewing the physical image quality metrics (SNR & CNR). At 70 and 75 kVp the CNR and SNR values were greater (~10%) than the reference image, across all additional fat thicknesses. When reviewing Figs. 4 and 5 there were a number of further trends noted when changing body part thickness on SNR and CNR. For 0–4 cm of additional fat, across all kVps, there was a slight reduction in SNR and CNR. Between 4 and 10 cm of additional fat, there was an increase in IQ (relative to the reference image) and then there was a marked decrease (step) in the physical IQ metrics between 10 and 15 cm of additional fat. Minor increases in additional fat could have been insignificant to cause changes in SNR and CNR up to 4 cm. After 4 cm, the AEC chambers could be better able to compensate for the increase in body part
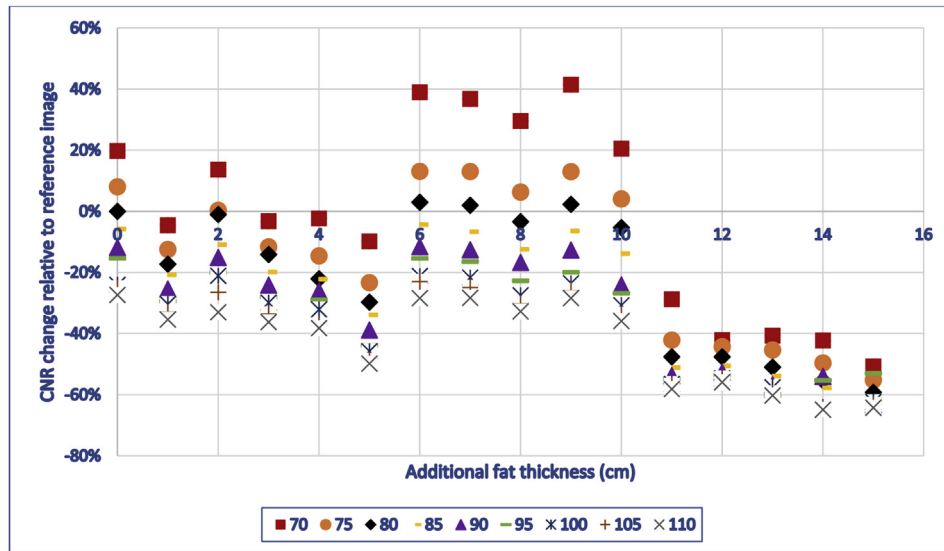
Figure 5. Percentage change of CNR relative to the reference image (80 kVp) for all body part thicknesses. Values in the figure legend correspond to the respective tube potentials.
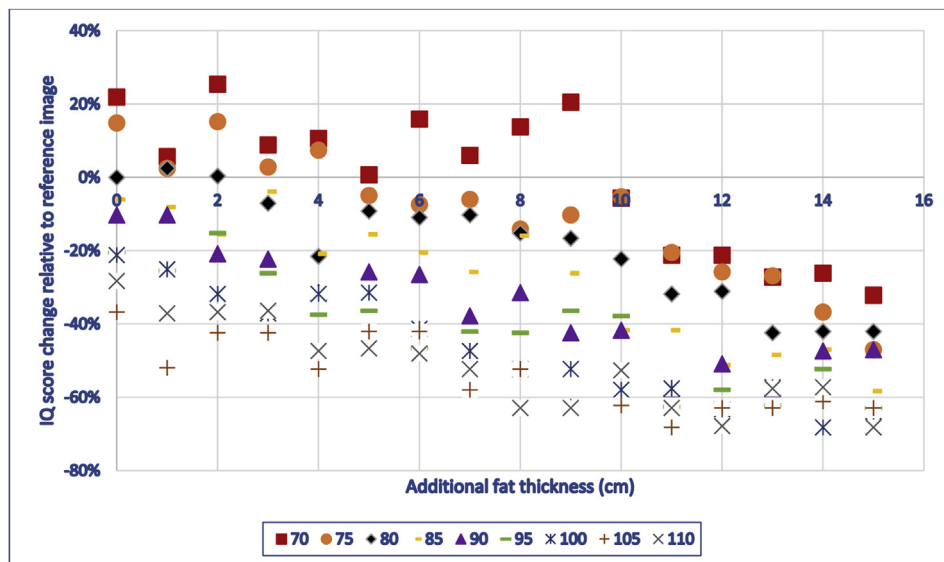

Figure 6. Percentage change of visual IQ relative to the reference image (80 kVp) for all thicknesses. Values in the figure legend correspond to the respective tube potentials.

thickness, this could also be supported by the post-processing ability of the DR system which was also able to compensate for an increase in exposure resulting in enhanced IQ. After 10 cm of additional fat there was a decrease in SNR and CNR; this may be due to an increase in the quantity of scattered radiation reaching the image receptor. It was also plausible that the image receptor and electronic post-processing were unable to effectively compensate for the increases in scattered radiation with 10 cm of additional fat in the primary beam and this also had a negative effect on IQ. We do accept that there could be alternative explanations for this trend but are unable to offer these at present. This trend was not clearly evidence on the visual IQ graph (Fig. 6) and this may result from physical measures of IQ (SNR & CNR) being more sensitive to subtle changes in IQ. It may have been useful to repeat the experiment to investigate whether this trend persisted, it would also be useful to consider investigating this within a wider programme of research projects to more fully understand changes in body part thickness

on digital radiography. Within Fig. 6 it was clear that as tube potential and body part thickness increased IQ declined.

Within the literature methods have been described to overcome the poor penetration of the X-ray photons, one such method is by increasing the kVp[6] but this was seen to have a resultant negative effect on IQ as a result of increased noise.[6] The increase in scattered radiation when using high tube potentials,[1] will also have a negative effect on the overall IQ. Furthermore, increasing the body part thickness increases the attenuation of the primary beam leading to a decrease in IQ as less photons reach the image receptor.[5,50]

Findings from our research were similar to Ullman et al.,[51] who found that SNR increased when using low tube potentials, however, they only investigated patients of an 'average' size and their study was distinctly different. Using lower kVps is recommended for several reasons, 1) DR detectors have high photon absorption levels, which are increased at low tube potentials. 2) The detector quantum efficiency (DQE) increases as the tube voltage is decreased. 3)

the k edge for DR is lower than that of film-screen which means an increase in image quality is seen for low tube voltages.[52] Research has indicated that using high tube potentials decreases the sensitivity of the phosphor plate. Fetterly and Hangiandreou[53] showed that the DQE of CR decreased when increasing the tube voltage (70—120 kVp).[53] A further explanation for decreases in IQ when the tube potential increases is due to higher mean energy of the X-ray photons. At higher energy levels the photon interaction moves away from predominantly the photoelectric effect to an increase in the proportion of interactions involving Compton scattering.[50] Within our results visual IQ scores decreased by more than 60% as body part thickness increased when using high tube potentials. The decrease was less than 20% when using 70 and 75 kVp, even for 15 cm of additional fat. Using 70 kVp provides a superior level of IQ when compared to the reference image when the fat thickness increased up to 10 cm.

The results from the radiographer's binary decision task, in which they evaluated the images from a general clinical practice perspective indicated that all experimental images were acceptable, and a clinical decision can be made regardless of the physical and visual measures. It should be acknowledged that the fat with consistently located in the same thickness across the phantom and in clinical practice differences may occur within specific anatomical regions, degrading the image further. But the results would indicate that even images obtained when using high tube potentials were sufficient. Since of the images were considered clinically acceptable across a wide range of acquisition factors, if we take dose into consideration, this means that using high tube potentials when imaging obese patients for pelvis radiography may be the optimum choice and promotes the ALARP principle, but further research is required.

To the authors' knowledge this is the first study to investigate the effect of different body part thicknesses on radiation dose and IQ for digital pelvic radiography. Two studies by Sebastian et al., in 2007 and 2008, explored the effect of patient size on IQ and patient dose when using CT.[54,55] Unsurprisingly, study results suggested that to maintain IQ at constant levels required higher radiation doses.[54]

Another study was conducted to identify the impact of imaging overweight and obese people on dose during radiographic examinations.[5] Within this phantom study chest and abdomen examinations were evaluated and five different body shapes were simulated. Findings were similar to our study. Increasing the radiation energy reduced the radiation dose, but adversely effected image contrast.[5] Adding 25 cm of the fat around the abdomen increased effective dose by 40 times. Our results indicate that by adding 15 cm fat the radiation dose increased by 156% at 70 kVp. However, when using 110 kVp the percentage dose difference between 0 cm and 15 cm was lower (37%).

Limitations

There are several limitations from our study. Using an anthropomorphic phantom is not fully representative of the human body since it lacks anatomical and pathological variation. Furthermore, the study was conducted using only a single digital radiography (DR) system and there are still some centres using computed radiography (CR) and/or alternative DR technologies. Tube potential was the only acquisition parameter investigated and greater understanding on the effects of SID, grid selection and AEC chamber configuration are warranted. Changes in the quantity of visceral fat between the organs was not included within the phantom design or dose modelling. We have reviewed the literature with regards to the use of PCXMC and similar Monte Carlo based dosimetry software. In the publication by Clark et al. (2010)

increasing phantom size was not shown to effect the position of internal organs and that they would only be covered by layers of adipose tissue.[26] The authors concluded that only minor differences in backscattered radiation would result. In their work it was clear that additional tissue was added to the periphery of the phantom (as in our work). We acknowledge that designing a computational model which simulates the additional fat geometry described in our work would be advantageous but would also be complex and require specialist computational expertise.

Conclusion

Acceptable IQ was evident across a wide range of acquisition factors, optimum IQ was obtained at 70 and 75 kVp for all fat thicknesses. This is at variance with professional practice where there is a tendency for radiographers to increase kVp as patient thickness increases. When radiation dose is a primary factor, the authors suggest that a high kVp could be used for radiography of the pelvis when presented with increase body part thickness.

Clinical indications for pelvis radiography should be carefully reviewed by the radiographer prior to the examination so that the optimum tube potential for the examination can be identified. If the clinical question requires a high level of detail e.g. primary pathology detection then images may be obtained at lower tube potentials whereas for follow-up a higher tube potential could reduce the dose but with a slight reduction in image quality, but still be diagnostic.

Conflict of interest statement

The authors declare no conflict of interest.

Acknowledgements

References

1. Carucci LR. Imaging obese patients: problems and solutions. *Abdom Imaging* 2013;**38**(4):630—46. https://doi.org/10.1007/s00261-012-9959-2.
2. Modica MJ, Kanal KM, Gunn ML. The obese emergency patient: imaging challenges and solutions. *Radiographics* 2011;**31**(3):811—23. https://doi.org/10.1148/rg.313105138.
3. Glanc P, O'Hayon BE, Singh DK, Bokhari SAJ, Maxwell CV. Challenges of pelvic imaging in obese women. *Radiographics* 2012;**32**(6):1839—62. https://doi.org/10.1148/rg.326125510.
4. Reynolds A. Obesity and medical imaging challenges. *Radiol Technol* 2011;**82**(3):219—39. http://www.ncbi.nlm.nih.gov/pubmed/21209424.
5. Yanch JC, Behrman RH, Hendricks MJ, McCall JH. Increased radiation dose to overweight and obese patients from radiographic examinations. *Radiology* 2009;**252**(1):128—39. https://doi.org/10.1148/radiol.2521080141.
6. Buckley O, Ward E, Ryan A, Colin W, Snow A, Torreggiani W. European obesity and the radiology department. What can we do to help? *Euro Radiol* 2009;**19**: 298—309.
7. Uppot RN, Sahani DV, Hahn PF, Gervais D, Mueller PR. Impact of obesity on medical imaging and image-guided intervention. *Am J Roentgenol* 2007;**188**(2): 433—40. https://doi.org/10.2214/AJR.06.0409.
8. Buckley O. Challenges of imaging the obese patient. *Irish Med Times* 2008;**42**(20):36.
9. IPEM. *Report 91: recommended standards for the routine performance testing of diagnostic X-ray systems*. 2005. York, http://hdl.handle.net/10454/6424.
10. Whitley A, Jefferson G, Hoadley G, Sloane C. *Clark's positioning in radiography*. 12th ed. London: Arnold: CRC Press; 2005. https://doi.org/10.1038/sj.bdj.4813067.
11. Despres J-P. Treatment of obesity: need to focus on high risk abdominally obese patients. *Br Med J* 2001;**322**(7288):716—20. https://doi.org/10.1136/bmj.322.7288.716.

12. Sturman-Floyd M. Moving and handling: supporting bariatric residents. *Nurs Resid Care* 2013;**15**(6):432–7. http://search.ebscohost.com/login.aspx?direct=true&db=ccm&AN=108017935&site=ehost-live.

13. Otto D, Ludwig K, Fessel A, et al. Digital selenium radiography: detection of subtle pulmonary lesions on images acquired with and without an additional antiscatter grid. *Eur J Radiol* 2000;**36**(2):108–14. https://doi.org/10.1016/S0720-048X(00)00265-5.

14. Neitzel U, Pralow T, Schaefer-Prokop CM, Prokop M. Influence of scatter reduction on lesion signal-to-noise ratio and lesion detection in digital chest radiography. *Med Imaging 1998 Phys Med Imaging* 1998;(April 2016):337. https://doi.org/10.1117/12.317033.

15. Bauer JS, Noël PB, Vollhardt C, et al. Accuracy and reproducibility of adipose tissue measurements in young infants by whole body magnetic resonance imaging. *PLoS One* 2015;**10**(2):1–12. https://doi.org/10.1371/journal.pone.0117127.

16. Valentine RJ, Misic MM, Kessinger RB, Mojtahedi MC, Evans EM. Location of body fat and body size impacts DXA soft tissue measures: a simulation study. *Eur J Clin Nutr* 2008;**62**(4):553–9. https://doi.org/10.1038/sj.ejcn.1602770.

17. Browne J, Watson A, Hoskins P, Elliott A, Watson AJ. Investigation of the effect of subcutaneous fat on image quality performance of 2D conventional imaging and tissue harmonic imaging. *Ultrasound Med Biol* 2005;**31**(7):957–64.

18. Glickman SG. Validity and reliability of dual-energy X-ray absorptiometry for the assessment of abdominal adiposity. *J Appl Physiol* 2004;**97**(2):509–14. https://doi.org/10.1152/japplphysiol.01234.2003.

19. Yoshizumi T, Nakamura T, Yamane M, et al. Abdominal fat: standardized technique for measurement at CT. *Radiology* 1999;**211**(1):283–6. https://doi.org/10.1148/radiology.211.1.r99ap15283.

20. Chan CTP, Fung KKL. Dose optimization in pelvic radiography by air gap method on CR and DR systems – a phantom study. *Radiography* 2015;**21**(3):214–23. https://doi.org/10.1016/j.radi.2014.11.005.

21. Manning-Stanley AS, Ward AJ, England A. Options for radiation dose optimisation in pelvic digital radiography: a phantom study. *Radiography* 2012;**18**(4):256–63. https://doi.org/10.1016/j.radi.2012.06.002.

22. Heath R, England A, Ward A, et al. Digital pelvic radiography: increasing distance to reduce dose. *Radiol Technol* 2011;**83**(1):20–8. http://ezproxy.fiu.edu/login?url=http://search.ebscohost.com/login.aspx?direct=true&db=rzh&AN=2011267440&site=ehost-live&scope=site.

23. Miyatake N, Matsumoto S, Miyachi M, Fujii M, Numata T. Relationship between changes in body weight and waist circumference in Japanese. *Environ Health Prev Med* 2007;**12**(5):220–3. https://doi.org/10.1265/ehpm.12.220.

24. Fontaine KR, Gadbury G, Heymsfield SB, Kral J, Albu JB, Allison D. Quantitative prediction of body diameter in severely obese individuals. *Ergonomics* 2002;**45**(1):49–60. https://doi.org/10.1080/00140130110112627.

25. Borrego D, Lowe EM, Kitahara CM, Lee C. Assessment of PCXMC for patients with different body size in chest and abdominal x ray examinations: a Monte Carlo simulation study. *Phys Med Biol* 2018;**63**:1–15. http://iopscience.iop.org/article/10.1088/1361-6560/aab13e/pdf [Accessed 21 June 2018].

26. Clark LD, Stabin MG, Fernald MJ, Brill AB. Changes in radiation dose with variations in human anatomy: moderately and severely obese adults. *J Nucl Med* 2010;**51**(6):929–32. https://doi.org/10.2967/jnumed.109.073015.

27. Li K, Bevins N, Zambelli J, Chen G-H. Model observer and human observer performance studies in differential phase contrast CT. *Med Imaging* 2013;**8668**:866817. https://doi.org/10.1117/12.2008102.

28. García-Pérez MA, Alcalá-Quintana R. Interval bias in 2AFC detection tasks: sorting out the artifacts. *Atten Percept Psychophys* 2011;**73**(7):2332–52. https://doi.org/10.3758/s13414-011-0167-x.

29. Merfeld DM. Signal detection theory and vestibular thresholds: I. Basic theory and practical considerations. *Exp Brain Res* 2011;**210**(3–4):389–405. https://doi.org/10.1007/s00221-011-2557-7.

30. Smedby Ö, Fredrikson M. Visual grading regression: analysing data from visual grading experiments with regression models. *Br J Radiol* 2010;**83**(993):767–75. https://doi.org/10.1259/bjr/35254923.

31. Båth M. Evaluating imaging systems: practical applications. *Radiat Prot Dosimetry* 2010;**139**(1–3):26–36. https://doi.org/10.1093/rpd/ncq007.

32. Hogg P, Blindell P. *Software for image quality evaluation using a forced choice method. United Kingdom Radiological Congress. Manchester.* 2012. p. 139.

33. Mraity H, England A, Cassidy S, Eachus P, Dominguez A, Hogg P. Development and validation of a visual grading scale for assessing image quality of AP pelvis radiographic images. *Br J Radiol* 2016;**89**(1061). https://doi.org/10.1259/bjr.20150430.

34. The Royal College of Radiologists. *Quality assurance in radiology reporting: peer feedback*, vol. 70. London: RCR; 2014. https://doi.org/10.1016/j.crad.2015.06.091.

35. Samei E, Dobbins J, Lo J, Tornai M. A framework for optimising the radiographic technique in digital x-ray imaging. *Radiat Prot Dosim* 2005;**114**(1–3):220–9.

36. Allen E, Hogg P, Ma WK, Szczepura K. Fact or fiction: an analysis of the 10 kVp 'rule' in computed radiography. *Radiography* 2013;**19**(3):223–7. https://doi.org/10.1016/j.radi.2013.05.003.

37. Sandborg M, Tingberg A, Ullman G, Dance DR, Alm Carlsson G. Comparison of clinical and physical measures of image quality in chest and pelvis computed radiography at different tube voltages. *Med Phys* 2006;**33**(11):4169–75. https://doi.org/10.1118/1.2362871.

38. Hess R, Neitzel U. Optimizing image quality and dose for digital radiography of distal pediatric extremities using the contrast-to-noise ratio. *RoFo Fortschr Geb Rontgenstr Neuen Bildgeb Verfahr* 2012;**184**(7):643–9. https://doi.org/10.1055/s-0032-1312727.

39. Martin CJ. Optimisation in general radiography. *Biomed Imaging Interv J* 2007;**3**(2). https://doi.org/10.2349/biij.3.2.e18.

40. Mori M, Imai K, Ikeda M, et al. Method of measuring contrast-to-noise ratio (CNR) in nonuniform image area in digital radiography. *Electron Commun Japan* 2013;**96**(7):32–41. https://doi.org/10.1002/ecj.11416.

41. Bloomfield C, Boavida F, Chabloz D, Crausaz E, Huizinga E. Experimental article – reducing effective dose to a paediatric phantom by using different combinations of kVp, mAs and additional filtration whilst maintaining image quality. *Optimax* 2014:81–4.

42. Desai N, Singh A, Valentino DJ. Practical evaluation of image quality in computed radiographic (CR) imaging systems. In: *Proc SPIE7622, Med Imaging Phys Med Imaging*, **1**(c); 2010. 76224Q. https://doi.org/10.1117/12.844640.

43. Lança L, Franco L, Ahmed A, et al. 10 kVp rule – an anthropomorphic pelvis phantom imaging study using a CR system: impact on image quality and effective dose using AEC and manual mode. *Radiography* 2014;**20**(4):333–8. https://doi.org/10.1016/j.radi.2014.04.007.

44. Alves AFF, Alvarez M, Ribeiro SM, Duarte SB, Miranda JRA, Pina DR. Association between subjective evaluation and physical parameters for radiographic images optimization. 2015. https://doi.org/10.1016/j.ejmp.2015.10.095.

45. Bushberg JT, Boone JM, Leidholdt EM, Boone JM. *The essential physics of medical imaging.* 2nd ed. Lippincott Williams & Wilkins; 2011. https://books.google.co.uk/books?hl=en&lr=&id=tqM8IG3f8bsC&oi=fnd&pg=PR1&dq=The+essential+Physics+of+medical+imaging&ots=9nkvXZlXkk&sig=DR2BLq1Gz8FqQUTip8IbtgTVBd0#v=onepage&q=The essential Physics of medical imaging&f=false [Accessed 19 July 2018].

46. Yap BW, Sim CH. Comparisons of various types of normality tests. *J Stat Comput Simul* 2011;**81**(12):2141–55. https://doi.org/10.1080/00949655.2010.520163.

47. Ghasemi A, Zahediasl S. Normality tests for statistical analysis: a guide for non-statisticians. *Int J Endocrinol Metab* 2012;**10**(2):486–9. https://doi.org/10.5812/ijem.3505.

48. Schroeder J, Reer R, Braumann KM. Video raster stereography back shape reconstruction: a reliability study for sagittal, frontal, and transversal plane parameters. *Eur Spine J* 2015;**24**(2):262–9. https://doi.org/10.1007/s00586-014-3664-5.

49. George D, Mallery P. *SPSS for windows step by step.* 4th ed. Boston, Mass, USA: Allyn & Bacon, Inc; 2000.

50. Egbe NO, Heaton B, Sharp PF. A simple phantom study of the effects of dose reduction (by kVp increment) below current dose levels on CR chest image quality. *Radiography* 2010;**16**(4):327–32. https://doi.org/10.1016/j.radi.2010.05.004.

51. Ullman G, Sandborg M, Tingberg A, Dance DR, Hunt R, Carlsson GA. Comparison of clinical and physical measures of image quality in chest PA and pelvis AP views at varying tube voltages. *Isrn* 2004;**98**:1102–799.

52. Tingberg A, Sjostrom D. Search for optimal tube voltage for image plate radiography. *Proc SPIE* 2003;**5034**:187. https://doi.org/10.1117/12.479982.

53. Fetterly KA, Hangiandreou NJ. Effects of x-ray spectra on the DQE of a computed radiography system. *Med Phys* 2001;**28**(2):241–9. https://doi.org/10.1118/1.1339883.

54. Schindera ST, Nelson RC, Toth TL, et al. Effect of patient size on radiation dose for abdominal MDCT with automatic tube current modulation: phantom study. *AJR Am J Roentgenol* 2008;**190**(2):100–5. https://doi.org/10.2214/AJR.07.2891.

55. Schindera ST, Nelson RC, Lee ER, et al. Abdominal multislice CT for obese patients: effect on image quality and radiation dose in a phantom study. *Acad Radiol* 2007;**14**(4):486–94. https://doi.org/10.1016/j.acra.2007.01.030.